

UNIVERSIDAD DE LOS ANDES

THESIS

Two-Photon Imaging Using Tunable Spatial Correlations

Author:
Juan VARGAS

Supervisor:
Dr. Alejandra VALENCIA

*A thesis submitted in fulfillment of the requirements
for the degree of Physicist*

in the

Quantum Optics
Physics Department



May 2, 2018

Declaration of Authorship

I, Juan VARGAS, declare that this thesis titled, "Two-Photon Imaging Using Tunable Spatial Correlations" and the work presented in it are my own. I confirm that:

- This work was done wholly or mainly while in candidature for a research degree at this University.
- Where any part of this thesis has previously been submitted for a degree or any other qualification at this University or any other institution, this has been clearly stated.
- Where I have consulted the published work of others, this is always clearly attributed.
- Where I have quoted from the work of others, the source is always given. With the exception of such quotations, this thesis is entirely my own work.
- I have acknowledged all main sources of help.
- Where the thesis is based on work done by myself jointly with others, I have made clear exactly what was done by others and what I have contributed myself.

Signed:

Date:

"Nonesenses... later due"

N.N

UNIVERSIDAD DE LOS ANDES

Abstract

Science Faculty
Physics Department

Physicist

Two-Photon Imaging Using Tunable Spatial Correlations

by Juan VARGAS

Two-Photon Imaging is a well studied phenomena, where we take advantage of the different correlations in which the light can be related to reconstruct the image of certain objects. In this Thesis use different spatial correlations of a SPDC light source, where we change this correlations changing the pump waist.

Acknowledgements

The acknowledgments and the people to thank go here, don't forget to include your project advisor...s

Contents

Declaration of Authorship	i
Abstract	iii
Acknowledgements	iv
1 Introduction	1
1.0.1 Computational Two-photon Imaging	1
2 Theory	3
2.1 Correlations between two photons	3
2.1.1 SPDC	3
2.1.1.1 Phase matching conditions	4
2.1.2 Spatial Correlations	5
2.1.3 Tunable Spatial Correlation SPDC source light	6
2.2 Imaging	6
2.2.1 Standar Imaging	7
2.2.2 Two-photon Imaging	7
2.2.2.1 Two-photon Imaging using entangled photon	8
2.2.2.2 Two-photon Imaging Using Chaotic Sources	11
3 Experimental Setup	12
3.1 SPDC Setup	12
3.1.1 Diode Laser	12
3.1.2 Mirror	12
3.1.3 Spatial Filter	12
3.1.4 Waist Lens	14
3.1.5 BBO(Beta Barium Borate) Crystal	15
3.2 Spatial Correlations Measurement Setup	15
3.2.1 Lens (Fourier Plane)	15
3.2.2 Polariser	16
3.2.3 Interferometer Filter	16
3.2.4 Pin Hole(Arduino)	16
3.2.5 Single Photon Counting Module(SPCM)	16
3.2.6 Field-programmable gate array(FPGA)	17
3.2.7 Computer(Data Analysis)	17
3.3 Two-Photon Imaging Setup	17
3.3.1 Mask	17
3.3.2 Folding Mirror	17
3.3.3 Bucket Detector	17

4 Results	19
4.1 Achiving a Gaussian Beam	19
4.2 Finding The Correlated Photons	19
4.3 Experimental Correlations	19
4.3.1 $w_p =?$	19
4.4 Mask Alignment	19
4.5 Two-Photon Images	20
4.5.1 mask1	20
4.5.2 mask2	20
4.5.3 mask3	20
5 Discussions and Conclusion	22
Bibliography	23

List of Figures

2.1	Simple Experimental setup for the SPDC process	4
2.2	Experimental Spatial correlations between a pair of down-converted photons. Right image shows the correlation in the x variable. Left shows the correlation in the y variable, Beam propagating in the z direction	6
2.3	Positive(A) and Negative(D) ideal spatial correlations	6
2.4	Optical imaging: a lens produces an image on an object at S_i . This distance is defined by the Gaussian thin-lens equation	7
2.5	Simple schematic for the Two-photon Imaging	8
2.6	Schematic of the first "two-photon imaging" experimental setup, used by Pittman[1]	9
2.7	The reflected photon, called signal	9
2.8	Experimental setup for the Two-photon imaging using thermal light, taken from [7]	11
3.1	Experimental Setup for the SPDC light Source	12
3.2	Image of the Diode Laser and it's control module, Taken from [2]	13
3.3	Mirror and the cavity mount	13
3.4	The spatial intensity profile before and after the spatial filtering process , Taken from [3]	14
3.5	Basic elements of a Spatial Filter. In our experiment we use a Aspheric Lens of $f = 30mm$ (LA1805-A), a pinhole of $50\mu m$ and a collimating lens of $f = 60mm$ (LA1134-A). Taken from [3]	14
3.6	This helps to form circular apertures of variable radius	14
3.7	Lens' effect on a Gaussian beam	15
3.8	Actual BBO crystal used in experiment	15
3.9	Experimental Setup for Obtaining the spatial correlations of a pair of down-converted photons	16
3.10	Single Photon Counting Module	16
3.11	Experimental Setup for the Two-photon Imaging	17
3.12	Foldind Mirror, it is in the position for measuring the correlations	18
4.1	We are moving the translational translational stage, to locate the spot where the correlated photon are, for this try me moved the y direction	19
4.2	Localization of the mask with an square	20
4.3	Moving the L Mask in order to put it in the most central spot	20
4.4	Long exposure of the definitive localization of the mask, in this try we leave the detector in each place for 30 seconds, we also make the steps of the detector smaller, $0.1mm$	21
4.5	Localization of the mask with an square	21

List of Tables

List of Abbreviations

LAH List Abbreviations Here
WSF What (it) Stands For

Physical Constants

Speed of Light $c_0 = 2.997\,924\,58 \times 10^8 \text{ m s}^{-1}$ (exact)

List of Symbols

a	distance	m
P	power	W (J s^{-1})
ω	angular frequency	rad

For/Dedicated to/To my...

Chapter 1

Introduction

Taking a photograph of an object, traditionally, we need to face a camera (detector) to the object. But with Two-photon imaging we use a detector that is towards the light source, rather than towards the object. As the name suggests it, Two-photon Imaging, we also use another photon that is strongly correlated.

Two-photon imaging has been demonstrated using two types of light sources. Type-one two-photon imaging uses entangled photon pairs as the light source. In 1995 Pittman, realized a quantum two-photon geometric optical effect. They have successfully performed optical imaging by means of a quantum-mechanical entangled source[1].

Type-two of imaging uses chaotic light. The type-two image-forming correlation is caused by the superposition between paired two-photon amplitudes, or the symmetrized effective two-photon wave-function[4].

1.0.1 Computational Two-photon Imaging

When we see the different setups shown here, (Figures 2.5, 2.6 and 2.8), it can be noted that the transmitted path of the light, consists of a light beam propagating through air. What differences these setup is the nature of the light used. Specially in the setup using thermal light, the transmitted path is a classical phenomenon that can be simulated by a computer using Fresnel's propagation theory. In Figure ?? we can see the setup for a Computational Two-photon Imaging, where the transmitted path of the light is replaced by a computational simulation generated by a computer.

The Computational Two-photon Imaging allows us to simulate the electric field data to be obtained before, during or after the data from the reflected arm is generated, eliminating the need for collecting the data generated in the transmitted path. Also we have to use less opto-electronical elements on the optical table, simplifying the original setup and reducing considerably the amount of data generated. The resulting detection module consists only in one detector, a bucket detector that collects a single pixel (no spatial information) on light which has been transmitted through or reflected from the object. In this situation only one light beam and one photodetector are required, this means that this imaging configuration cannot depend on non-local two-photon interference.

Even though this realisation of the Two-photon Imaging is relevant in this discussion, because it is possible to retrieve the image by precomputing the intensity fluctuation pattern that would have been seen by a high-spatial-resolution detector in a lensless two-photon imaging. It means we introduced some kind of coherence in this single path two-photon imaging. This is done by putting a CW laser beam through a spatial light modulator (SLM) whose inputs are chosen to create the desired coherence behavior[8]. A SLM is a special device that can manipulate light

by modulating the amplitude, phase or polarization of the light waves in the two dimensions of space and time.

Chapter 2

Theory

In Here we will discuss some important facts to get a complete understanding in the physical phenomena that is happening. Specially we will develop the notions that are crucial in the understanding of the Two-photon imaging using entangled light, been this said we will start talking about correlations.

2.1 Correlations between two photons

The term "correlation" is crucial at this point, and it refers to the relation of two or more situations have. For example we can establish a correlations between the US dollar currency exchange rate and the prices of technology in one country. These two things have direct relation, if one blows up, the other one will too. These two situations, or variables, can have a strong correlations or a week one.

Indeed in quantum physics we can have a pair of photons that are so strongly correlated, in their possible variables (spatial and temporal), that we say they are entangled. This statement can leads us to a dense discussion about the nature of this entanglement, a discussion that were started between Einstein and Bohr in the first years of quantum physics [9].

To avoid this discussion we will just talk about correlations, and when referring about a pair of correlated photons, we will mean that this pair of photons are correlated in one or varius of their variables. They can be correlated in momentum, meaning that when one photon have a given \vec{q}_i momentum and the other photon have a \vec{q}_j momentum that is determined by the first, this relations is the momentum correlations a we can work out an expression for this relationship.

2.1.1 SPDC

As the title of this work implies, we need a source light that produces pair of photons, and we would like to exploit the advantages of strong correlations between them. The photons generated via spontaneous parametric down conversion (SPDC) are widely used in quantum optics experiments. The popularity of this source of paired photons is strongly related to the relative simplicity of its experimental realisation, and to the variety of quantum features that down converted photons can exhibit. The generated photons via SPDC can be correlated in different degrees of freedom, for example in polarisation, in frequency and in the equivalent degrees of freedom: 'orbital angular momentum, space and transverse momentum [10].

SPDC is an optical process in which focus a beam pump, that is propagating in the z-direction, to a nonlinear crystal of length L . Using first order perturbation and

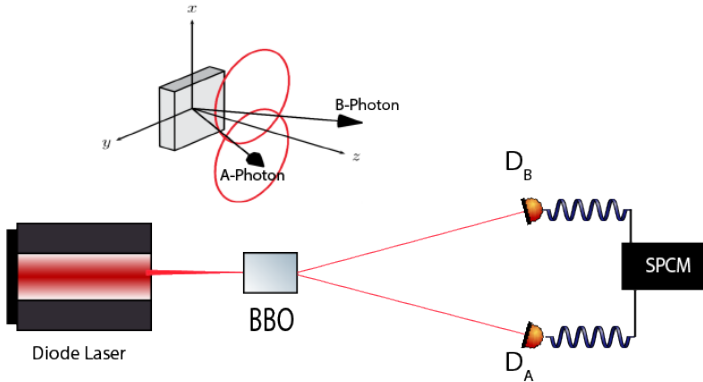


FIGURE 2.1: Simple Experimental setup for the SPDC process

in the paraxial approximation, the two-photon state is given by:

$$|\Psi\rangle = \int dq_B dq_A d\Omega_B d\Omega_A x [\Phi(q_B, \Omega_B; q_A, \Omega_A) \hat{a}^\dagger(\Omega_B, q_B) \hat{a}^\dagger(\Omega_A, q_A) + \Phi(q_A, \Omega_A; q_B, \Omega_B) \hat{a}^\dagger(\Omega_B, q_B) \hat{a}^\dagger(\Omega_A, q_A)] |0\rangle \quad (2.1)$$

Where this state function depends on the transverse wave vectors $q_n = (q_n^x, q_n^y)$ and frequency detuning, $\Omega_n = \omega_n - \omega_0^n$, around the central frequencies, ω_0^n , for the photon at the path A or B ($n = A, B$). The $\Phi(q_B, \Omega_B; q_A, \Omega_A)$ and $\Phi(q_A, \Omega_A; q_B, \Omega_B)$ are the mode functions or biphotons that contains all the informations about the correlations between the pair of down-converted photons. The operator \hat{a}^\dagger indicates the creations of an n -polarized photon with transverse momentum q_n , and frequency detuning Ω_n [4].

In the optical table we put a polariser at certain directions at the detections modules, filtering some of the photons before reaching the detector, this filtering also have a mathematical effect in our model, it is possible now to write 2.1 different, dropping one term:

$$|\Psi\rangle = \int dq_B dq_A d\Omega_B d\Omega_A x [\Phi(q_B, \Omega_B; q_A, \Omega_A) \hat{a}^\dagger(\Omega_B, q_B) \hat{a}^\dagger(\Omega_A, q_A)] |0\rangle \quad (2.2)$$

The mode function $\Phi(q_B, \Omega_B; q_A, \Omega_A)$ is related with the joint probability of detecting both an B -polarized photon, with tranverse momentum q_B and frequency detuning Ω_B , at the detector B and an A -polarized photon, with tranverse momentum q_A and frequency detuning Ω_A , at the detector A .

2.1.1.1 Phase matching conditions

In particular, $\Phi(q_B, \Omega_B; q_A, \Omega_A)$ reads [10]:

$$\Phi(q_B, \Omega_B; q_A, \Omega_A) = \mathcal{N} \alpha(\Delta_0, \Delta_1) \beta(\Omega_B, \Omega_A) \times \text{sinc}\left(\frac{\Delta_k L}{2}\right) e^{i \frac{\Delta_k L}{2}} \quad (2.3)$$

Where \mathcal{N} is a normalisation constant, $\alpha(\Delta_0, \Delta_1)$ and $\beta(\Omega_B, \Omega_A)$ yields the informations of the pump's transverse and spectral distribution, respectively, L is the length of the nonlinear crystal. For the process that is happening inside the crystal, there are some conditions that have to be fulfilled. These conditions are related with the energy and momentum conservations inside the parametric down conversion process. The terms Δ_0 , Δ_1 and Δ_k are functions that result from the phase matching

conditions and read:

$$\Delta_0 = q_B^x + q_A^x \quad (2.4)$$

$$\Delta_1 = q_A^y \cos\phi_A + q_B^y \cos\phi_B - N_B \Omega_B \sin\phi_B + N_A \Omega_A \sin\phi_A - \rho_B q_B^x \sin\phi_B \quad (2.5)$$

$$\Delta_k = N_p(\Omega_B + \Omega_A) - N_B \Omega_B \cos\phi_B - N_A \Omega_A \cos\phi_A - q_B^y \sin\Omega_B + q_A^y \sin\Omega_A + \rho_p \Delta_0 - \rho_B q_B^x \cos\phi_B \quad (2.6)$$

The angles ϕ_B and ϕ_A are the creation angles of the down- converted photons inside the crystal with respect to the pump's propagation direction, whereas the angles ρ_p and ρ_B account for the walk-off of the pump p and the B down- converted photon, respectively. In this study, ϕ_B and ϕ_A are treated as constants, mainly because the scanned transverse momentum regions represent a small portion around the emission angles. N_h denotes the inverse of the group velocity for each photon.

2.1.2 Spatial Correlations

In order to observe the correlations presented in 2.3 we have to take into account some considerations about the description of the things we have in optical table. First of all we have a pump beam with a Gaussian profile with waist w_p in such way that $\alpha(\Delta_0, \Delta_1) \propto \exp[-w_p^2(\Delta_0^2 + \Delta_1^2)/4]$, a CW pump laser, mathematically represented by $\beta(\Omega_B, \Omega_A) \propto \delta(\Omega_B + \Omega_A)$. Making the approximations for the sinc function by a Gaussian functions with the same width at $1/e^2$ of its maximum, i.e., $\text{sinc}(x) \approx \exp(-\gamma x^2)$ with γ equal 0.193. The mode function reduces to:

$$\Phi(q_B, \Omega_B; q_A, \Omega_A) = \mathcal{N} \beta(\Omega_B, \Omega_A) \times \exp \left[-\frac{w_p^2(\Delta_0^2 + \Delta_1^2)}{4} - \gamma \left(\frac{\Delta_k L}{2} \right)^2 + i \frac{\Delta_k L}{2} \right] \quad (2.7)$$

In order to observe the transverse correlations (spatial correlations), the frequency information has to be traced out, in the optical table this can be achieved by placing some interferometer filters before detection. This spectral filters are modeled as $f_n(\Omega_n) = \exp[-\Omega_n^2/(4\sigma_n^2)]$, with bandwidth σ_n chosen to achieve a regimen where the spatial-spectral correlations are completely broken [11]. To achieve this mathematically we have to integrate 2.7 around the spatial variables:

$$\tilde{\Phi}(q_B, q_A) = \int d\Omega_B d\Omega_A f_B(\Omega_B) f_A(\Omega_A) \Phi(q_B, \Omega_B; q_A, \Omega_A) \quad (2.8)$$

Figure 2.2 show a couple of examples of how these correlations we are talking about look like. These correlations have some kind of circular shape, and show how strong is the possibility of detecting a photon at a given position, looking at the first graph, there is a great chance of detecting simultaneously a photon at $x_B = 0$ and at $x_A = 0$. Now if we look at the left graph, it is showing the correlation of the pair of photons in the y direction, there is a significant probability of measuring simultaneously a photon at $y_B = 0.4$ and at $y_A = -0.4$. It is interesting how in this case there is a "negative" correlation, the expected position at which we will find the other photon, is at the same, but negative position. Another interesting fact we have to point out, is that this correlations also can be sharper, the x correlation have a more circular shape, making wider the possible values for a given x_B . In contrast the y correlation is more elliptic, meaning it restricts the possible values for a given y_B . It is easy to think how a strong correlation should look like, a strong correlations in spatial variables would mean that if we have the position of one photon at the

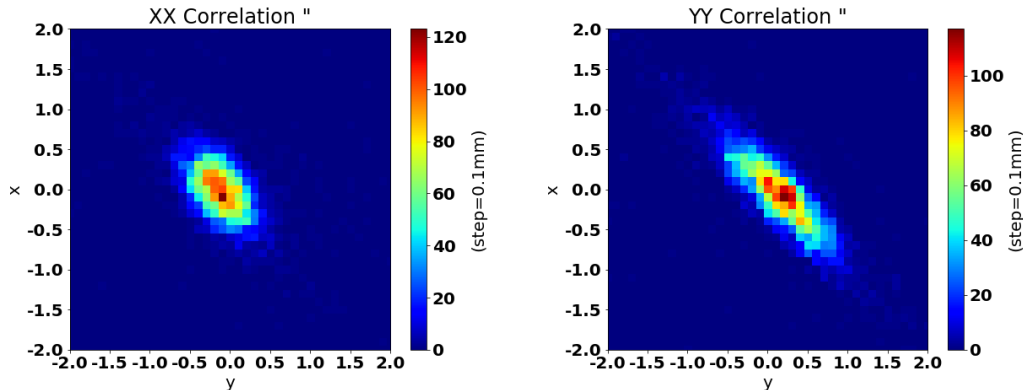


FIGURE 2.2: Experimental Spatial correlations between a pair of down-converted photons. Right image shows the correlation in the x variable. Left shows the correlation in the y variable, Beam propagating in the z direction

position x_B we immediately would know which x_A have the other photon, this kind of ideal spatial correlation would look like a straigh line really thin, Figure ??.

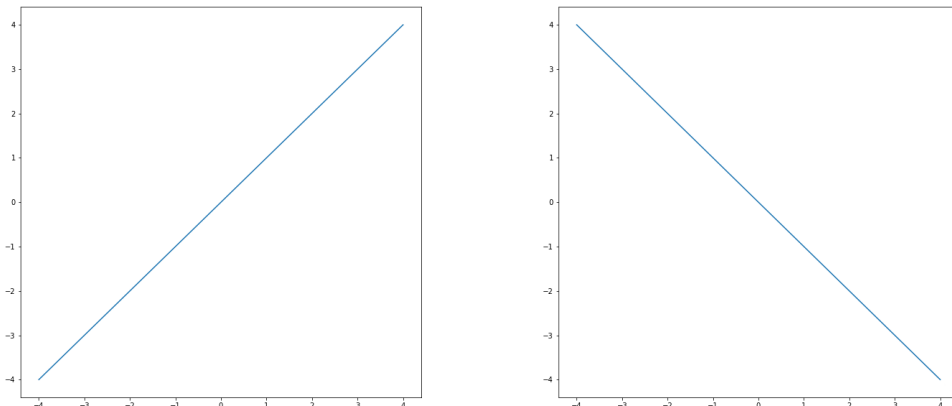


FIGURE 2.3: Positive(right) and Negative(left) ideal spatial correlations

2.1.3 Tunable Spatial Correlation SPDC source light

It is clear that both 2.7 and 2.8 depend on w_p , the pump waist. If we change this parameter and keep the rest of the parameters constant, the term in the exponential function $[-w_p^2(\Delta_0^2 + \Delta_1^2)/4]$ will variate, making changes in the shape of the original mode function. As it was mentioned here before and in [12], the mode function contains all the informations about the correlations of the generated down converted photons. Hence changing the pump waist w_p will change the correlations of the generated pair of photons.

2.2 Imaging

Assuming we have an object that have its own light or its externally illuminated, imaging means collecting that light that is emitted from the object. Each point of the surface of the object will emit spherical waves to all possible directions, being this said, What is the probability to have a spherical wave collapsing into a point or small spot? Obviously, the chance is practically zero unless an imaging system is applied. The concept of optical imaging was well developed in classical optics and the Figure 2.4 schematically illustrates a standar imaging setup. In this setup an object is illuminated by a radiation source, an imaging lens is used to focus the scattered and reflected light from the object onto an image plane which is defined by the “Gaussian thin lens equation”[5]:

$$\frac{1}{S_0} + \frac{1}{S_i} = \frac{1}{f} \quad (2.9)$$

where S_0 is the distance between the object and the imaging lens, S_i the distance between the imaging lens and the image plane, and f the focal lenght of the imaging lens. This equation defines a point-to-point relationship between the object plane and the image plane: any radiation starting from a point on the object will colapse at a certain point at the image plane.

This one-to-one correspondence in the image-forming relationship between the

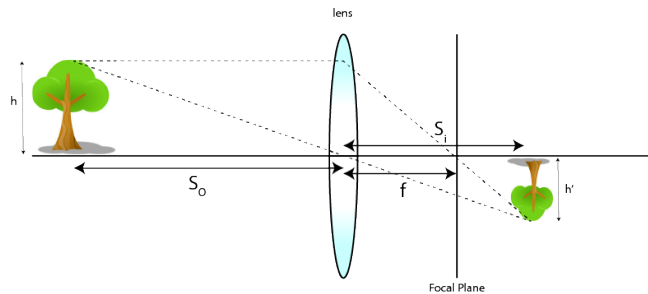


FIGURE 2.4: Optical imaging: a lens produces an image on an object at S_i . This distance is defined by the Gaussian thin-lens equation

object and the image planes produces a perfect image. The observed image can be magnified or demagnified, for example, in the Figure 2.4 the original object is a tree, and it is demagnified at the image plane. This depends on which optical system are we using, what kind on lenses are involved and the distance between object and them.

2.2.1 Standar Imaging

The observed image is a reproduction of the illuminated object, mathematically corresponding to a convolution between the object distribution fuction $|T(\vec{\rho}_o)|^2$ (aperture function) and a δ -function, which is present for the perfect point-to-point correspondence [13]:

$$I(\vec{\rho}_i) = \int_{obj} d\vec{\rho}_o |T(\vec{\rho}_o)|^2 \delta(\vec{\rho}_o + \frac{\vec{\rho}_i}{m}) \quad (2.10)$$

where $I(\vec{\rho}_i)$ is the intensity at the image plane, $\vec{\rho}_o$ and $\vec{\rho}_i$ are 2-D vectors of the transverse coordinates in the object and image planes, respectively, and $m = s_i/s_o$ is the image magnification factor.

In reality, we are limited by the finite size of the optical system, we may never obtain a perfect image. we have to take into account the constructive-destructive interference present in this phenomena, because of the wave nature of light. The point-to-point correspondence turns into a point-to-'spot' relationship. For further informations about this "real life" situation check the ??.

2.2.2 Two-photon Imaging

Two-photon imaging consist after all, in reconstructing an image of an object. But in this case we use two dectector located in differents paths of the light. By using the detections of them separately we get a constant signal, with no information about the object, Figure 2.5. But if instead we use the signal of them both, counting coincidences, we can reconstruct the double slit in Figure 2.5.

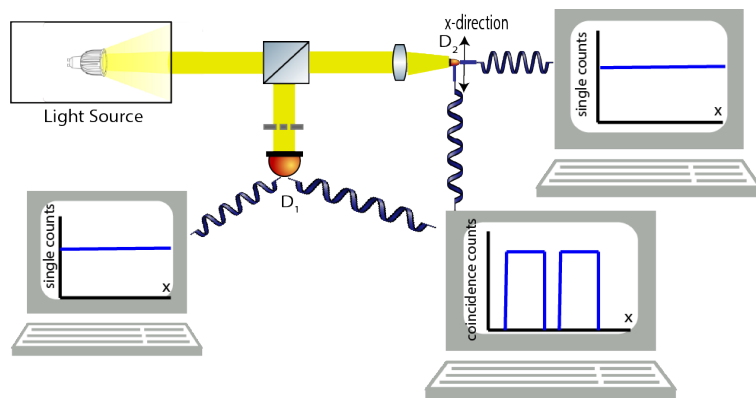


FIGURE 2.5: Simple schematic for the Two-photon Imaging

In order to reconstruct the image of the double slit, we have to introduce some kind of spatial dependence, the object, in this case the double slit, is distributed along a transverse direction of the light propagation. But what we have learnt is that scanning along the x-direction (assuming that light propagates along the z-direction), in the path that have no interaction with the object D_2 , and collecting all the light that interacts with the object D_1 , gathering no spatial information. We reconstruct the double slit in the coincidences counts, every time we have a photon detected going through the double slit, and a photon at a certain position x_i , we graph coincidences vs x_i and we get the image of the double slit, Figure 2.5.

The optical imaging used the photons at the image plane, to form the image. In other words it takes measure one photon per spot at the image plane. For the type-one and type-two two-photon imaging, in certain aspects the behaviour is similar as that of the classical. They both exhibit a similar point-to-point imaging-forming function, except the two-photon image is only reproducible in the joint-detection between two independent photodetectors, and the point-to-point imaging-forming function is in the form of second-order correlation,

$$R_{12}(\vec{\rho}_i) = \int_{obj} d\vec{\rho}_o |T(\vec{\rho}_o)|^2 G^{(2)}(\vec{\rho}_o, \vec{\rho}_i) \quad (2.11)$$

where $R_{12}(\vec{\rho}_i)$ is the joint-detection counting rate between photodetectors D_1 and D_2 . $G^{(2)}(\vec{\rho}_o, \vec{\rho}_i)$ is a nontrivial point-to-point second-order correlation function, corresponding to the probability of observing a joint photo-detection event at the coordinates $\vec{\rho}_o$ and $\vec{\rho}_i$. The physics behing $G^{(2)}(\vec{\rho}_o, \vec{\rho}_i)$ is what changes between type-one

and type-two two-photon imaging.

2.2.2.1 Two-photon Imaging using entangled photon

In the previous section we introduced the notion of two-photon imaging , but we didn't care much about the nature of the source light. For this case we will use entangled photon as the source light, we will separate the pair of entangled photons by means of a polarization beamsplitter. The first type-one two-photon imaging experiment was demonstrated by Pittman in 1995[1]. The schematic setup of the experiment is shown in the Figure 2.6.

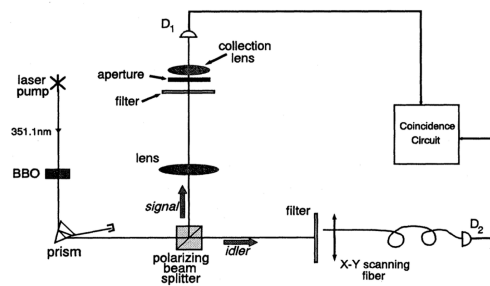


FIGURE 2.6: Schematic of the first "two-photon imaging" experimental setup, used by Pittman[1]

A continuous wave (CW) laser is used to pump a nonlinear crystal to produce pairs of entangled photons. This pairs of orthogonally polarized signal and idler photons are the product of the nonlinear optical process of spontaneous parametric down-conversion (SPDC). The pair emerges from the crystal collinearly¹, it is separated by a dispersion prism, and then the signal and idler are sent in different directions by a polarization beam slitting Glan-Thompson prism.

The reflected signal beam passes through a convex lens with a 400mm focal length and illuminates an aperture². Before the aperture is placed a filter (Figure 2.7), this is a bandwidth spectral filters centered at the wavelength 702.2nm. Behind the aperture is the detector package D_1 .

¹The pairs emerge from the crystal nearly collinearly, with $\omega_s \simeq \omega_i \simeq \omega_p/2$. where the subscript letter stands for signal, idler and pump respectively

²The aperture consisted of the letters UMBC, University of Maryland Baltimore County.

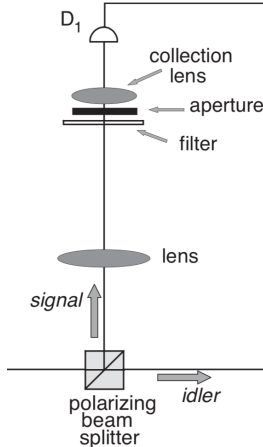


FIGURE 2.7: The reflected photon, called signal

The transmitted idler beam is met by detector package D_2 . The input tip of the fiber is scanned in the transverse plane. The counts are sent to a coincidence counting circuit with a 1.8ns acceptance window.

An important fact of this experiment is the use of a lens(collection lens) in the signal beam that establishes an image plane with the definitive point-by-point correspondence object(mask) plane.

The Biphoton then takes a quadratic form:

$$\tilde{\Phi}(q_s, q_i) = N \exp \left[-\frac{1}{2} x^T A x + i b^T x \right] \quad (2.12)$$

where N is a normalization constant, x is a 4-dimensional vector defined as $x = (q_s^x, q_s^y, q_i^x, q_i^y)$, A is a 4×4 real-valued, symmetric, positive definite matrix and b is a 4-dimensional vector. A and b are defined from the phase-matching conditions of the SPDC process. x^T and b^T denote the transpose of x and b . A and b are functions that depend of all the relevant parameters in the experiment such as the length of the crystal L , pump waist w_p , creation angles inside the crystal φ_n and the width of the spectral filter σ_n .

A way to quantify the degree of spatial correlation we shall define 'correlation parameter':

$$K^\lambda = \frac{C_{si}^\lambda}{\sqrt{C_{ss}^\lambda C_{ii}^\lambda}} \quad (2.13)$$

calculated for each direction ($\lambda = x, y$) from the covariance matrix C^λ with elements $C_{kj}^\lambda = \langle q_k^\lambda q_j^\lambda \rangle - \langle q_k^\lambda \rangle \langle q_j^\lambda \rangle$.

Fresnel Propagator

Fresnel Propagator: $h(r, z) = (-\frac{i}{\lambda z}) e^{(i\frac{2\pi z}{\lambda})} \Psi(r, z)$ with $\Psi(r, z) = e^{(i\frac{\pi}{\lambda z})r^2}$. Thin-lens transfer function $L_f(r) = \Psi(r, -f)$

$$G = \int d^2 r_1 \int d^2 r_0 h(r_f - r_1, f) L_f(r_1) h(r_1 - r_0, f) \quad (2.14)$$

The propagation is done by determining the Green function[14] of the optical path by which the beam will travel. The biphoton function in terms of transverse

momenta $\Phi_1(q_s, q_i)$ after traveling through two arbitrary optical paths can be expressed in terms of the corresponding Green functions and the initial biphoton function $\Phi(q_s, q_i)$ as:

$$\Phi_1(q_s, q_i) = G_s(q_s, r_1)G_i(q_i, r_2)\Phi(q_s, q_i) \quad (2.15)$$

$$\Phi_1(r_1, r_2) = \int d^2q_s d^2q_i \Phi_1(q_s, q_i) \quad (2.16)$$

Taking advantage of the 2-F system as a Fourier-Transform to reduce the amount of calculations. Solving 2.14 over r_0 and r_1 we have:

$$G(q, r_f) = Ce^{\frac{i\pi}{\lambda f}r_f^2}e^{\frac{i\lambda f}{4\pi}q^2}\delta(q - \frac{2\pi}{\lambda f}r_f) \quad (2.17)$$

where C is a complex constant that depends only on $\lambda = 2\pi c$ and f . Then we can define the Green Functions for each path:

$$G_1(q_s, r_1) = G(q_s, r_1)xT(r_1) \quad (2.18)$$

$$G_2(q_i, r_2) = G(q_i, r_2) \quad (2.19)$$

Where $T(r_1)$ is the transfer function of the object.

Gathering all the previous results we can obtain $\Phi_1(r_1, r_2) = C^2T(r_1)\Phi(\frac{2\pi}{\lambda f}r_1, \frac{2\pi}{\lambda f}r_2)$, which describes the biphoton at the planes of the object and the scanning detector. It shows that the biphoton at the 2F plane in terms of r_1 and r_2 has the same form as the biphoton at the output face of the crystal with the relationship $q = \frac{2\pi}{\lambda f}r$. This allows to computationally simulate the biphoton at the 2-F plane by using Eq 2.12 without the need to computationally simulate its propagation through the 2-F system.

We are collecting all the light that interacts with the object by the means of a bucket detector, this from the mathematical point of view leave us with: $\Phi_1(r_2) = C^2 \int d^2r_1 T(r_1)\Phi(\frac{2\pi}{\lambda f}r_1, \frac{2\pi}{\lambda f}r_2)$ The coincidence counts that will be measured by the Detectors will be proportional to the magnitude square of the resulting biphoton function $\Phi_1(r_2)$.

$$S(r_2) \propto |\int d^2r_1 T(r_1)\Phi(\frac{2\pi}{\lambda f}r_1, \frac{2\pi}{\lambda f}r_2)|^2 \quad (2.20)$$

For non-ideal forms of $\Phi(q_s, q_i)$ we have the relation between $\Phi(q) \rightarrow \Phi(r)$ for a 2F system, Hence: $\Phi(r) = \frac{1}{\sqrt{\det(\Sigma)(2\pi)^4}}e^{-\frac{1}{2}r^T\Sigma^{-1}r}e^{ibr}$
 $\Sigma =$

2.2.2.2 Two-photon Imaging Using Chaotic Sources

In principle the term "thermal radiation" should refer only to radiation coming from a blackbody in thermal equilibrium at some temperature T. But with this realisation of thermal radiation we have to face some characteristics of true thermal fields. Thermal radiation is also referred as chaotic light, which have extreme short coherence time. *expand coherence time*

Thermal sources have to be understood as incoherent light, this means that we have many photons at the beam, but the frequencies they have are randomly distributed. In the case of entangled light, we had a light source that generated photons that all are around a given frequency, we used a diode laser at 405nm.

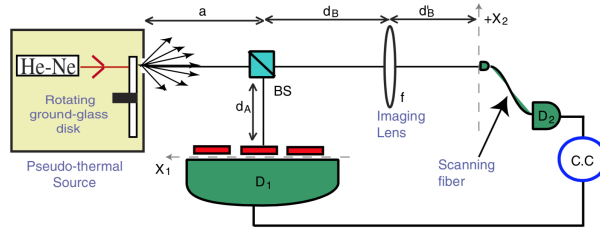


FIGURE 2.8: Experimental setup for the Two-photon imaging using thermal light, taken from [7]

The source light in Figure 2.8 is the one developed by Martinssen and Spiller[6] which is the most commonly used among the pseudothermal fields. A coherent laser radiation is focused on a rotating ground glass disk, the scattered radiation is chaotic with a Gaussian spectrum.

It is possible to establish an analogy between classical optics and entangled two-photon optics: the two-photon probability amplitude plays in entangled two-photon processes the same role that the complex amplitude of the electric field plays in classical optics [7].

Chapter 3

Experimental Setup

3.1 SPDC Setup

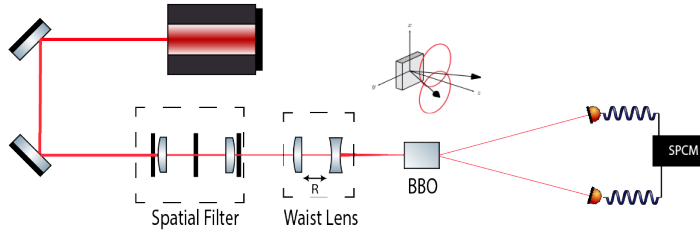


FIGURE 3.1: Experimental Setup for the SPDC light Source

3.1.1 Diode Laser

The light source used in this experiment is a Diode Laser that delivers a continuous wave(CW) at $\lambda = 406,101\text{nm}$ and $\Delta\lambda = 4\text{nm}$. The laser model No. DL 405-200 delivers light at 200 mW with a beam diameter of 1.5 mm and a beam Divergence 1.2 mrad. IN HERE I MAY TALK ABOU THE M FACTOR, QUALITY PARAMETER OF GAUSIAN BEAMS M^2 Power 200mW

3.1.2 Mirror

further details to be asked,

3.1.3 Spatial Filter

A laser beam can be characterized by measuring its spatial intensity profile at points perpendicular to its direction of propagation. The spatial intensity profile is the variation of intensity as a function of distance from the center of the beam, in a plane perpendicular to its direction of propagation. In the Figure 3.4(top part) we see the input gaussian beam and how its intensity fluctuates around the x axis. The output desired beam after going through the spatial filter is shown at the bottom of the Figure 3.4. The simplest arrangement to achieve this output spatial intensity profile is show in the Figure 3.5, where at the end we have a beam which intensity strength falls off transversely following a bell-shaped curve that's symmetrical around the central axis. Taking a closer look at the Figure 3.4(top part) we may recognise a diffraction pattern, but when we measure this spatial profile directly from the diode laser, we find out that it doesn't follow that behaviour, on the contrary it follows



FIGURE 3.2: Image of the Diode Laser and it's control module, Taken from [2]



FIGURE 3.3: Mirror and the cavity mount

a more random spatial profile. This ramdom spatial profile is a result of the randomness in the quantum emissions and absorptions that are happening at the exited atoms at the diode laser[5].

In order to have this spatial intensity profile at the input of my lens arrangement, Figure 3.5, we put a circular aperture with the help of a pair of irises, Figure 3.6,

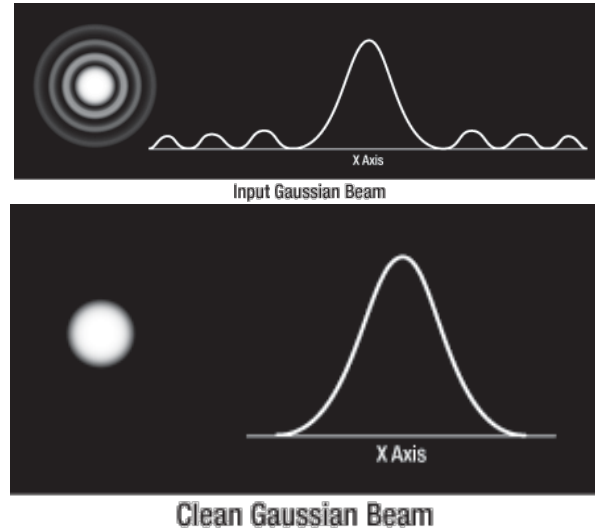


FIGURE 3.4: The spatial intensity profile before and after the spatial filtering process , Taken from [3]

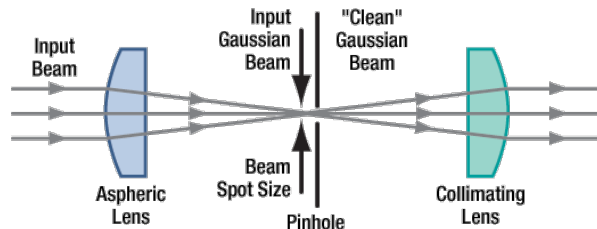


FIGURE 3.5: Basic elements of a Spatial Filter. In our experiment we use a Aspheric Lens of $f = 30\text{mm}$ (LA1805-A), a pinhole of $50\mu\text{m}$ and a collimating lens of $f = 60\text{mm}$ (LA1134-A). Taken from [3]

before the $f = 30.0\text{mm}$ lens and after the $f = 60.0\text{mm}$ lens.



FIGURE 3.6: This helps to form circular apertures of variable radius

3.1.4 Waist Lens

A Gaussian beam hits a lens....To control the pump waist we can put a lens in the propagation direction with certain focal lenght f . This lens will define a zone around the distance f called *Focus depth*[5] , where in the middle we find the narrowest point of the beam, Figure 3.7. The radius of this zone is:

$$W_0 = \frac{\lambda f}{\pi W_B} \quad (3.1)$$

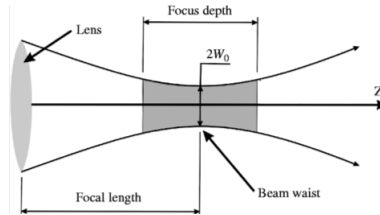


FIGURE 3.7: Lens' effect on a Gaussian beam

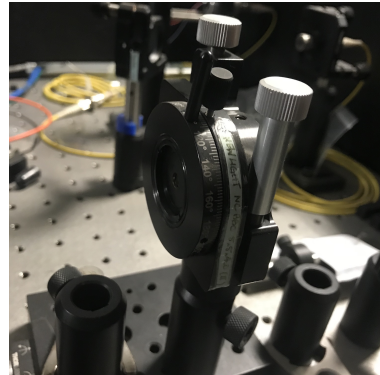


FIGURE 3.8: Actual BBO crystal used in experiment

Where W_B is the initial waist beam.

If we want to focus the beam at a fixed distance F , using this method to control the pump waist is not practical. Every different lens we would use will make this waist W_0 at different distances f . It is necessary to find a *Waist lens* that makes us a waist W_0 at a transverse plane located in a fixed position F from the *Waist Lens*. This special lens consists in an arrangement of two lenses, a positive and negative one respectively, separated a distance d_0 from each other. SOURCE WHERE THEY EXPLAIN HOW TO USE A POSITIVE AND NEGATIVE ASK OMAR!!!

3.1.5 BBO(Beta Barium Borate) Crystal

the power of the pump is 60mW The nonlinear optical media used in this experiment is a BBO(Beta Barium Borate) crystal, this crystal is 5x5x4mm. BBO ($\beta\text{-BaB}_2\text{O}_4$) The crystal is mounted in such way that the input and output plane are fixed, Figure 3.8.

3.2 Spatial Correlations Measurement Setup

From this point we will talk about a pair of entangled photon pairs, that will come from the output plane of the BBO crystal, for historical reasons we will label this pairs as *signal* and *idler*.

3.2.1 Lens (Fourier Plane)

To define the $2f$ system we use a lens(LA1708) of $f = 200.0\text{mm}$ in front of each *signal* and *idler*. This lens is placed at a distance f from the output plane.

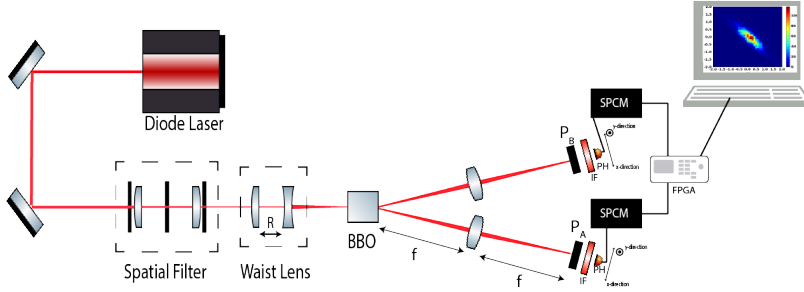


FIGURE 3.9: Experimental Setup for Obtaining the spatial correlations of a pair of down-converted photons

3.2.2 Polariser

In order to be able to filter certain polarisation direction we used a pair of Polarisers(WP25M-UB), which consist in a circular surface than only transmit the light that comes in a specific direction. other directions are reflected

3.2.3 Interferometer Filter

In this situation we are interested in the correlations in the space variables, hence we would like to filter al this time variables. To do this filtering we used a spectral filter(FB810-10) that only transmits the light that comes with $\lambda = 810 \pm 2nm$.

3.2.4 Pin Hole(Arduino)

MORE DETAILS, HOW MANY ARDUINOS, coupling lens refernece ETC ...

3.2.5 Single Photon Counting Module(SPCM)

To detect photons we a self-contained module that detects single photons of light over the $400nm$ to $1069nm$ wavelength range. The module used (SPCM-AQRH-13) uses a unique silicon avalanche photodiode (SLiK) with a detection efficiency of more than 65%[15]. Light is transmitted through a optic fiber from the pin hole detector to the SPCM. The result signal coming from the SPCM are pulses that represents one photon detections.



FIGURE 3.10: Single Photon Counting Module

3.2.6 Field-programmable gate array(FPGA)

Both *signal* and *idler* pulses from the respective SPCM goes to the same FPGA(ZestSC1). This Field-programmable gate array is programmed to count the photon coincidences, this means that the FPGA is fast enough to detect and separate pulses from photons that are time-separated.

3.2.7 Computer(Data Analysis)

labview is used to control the detection module, where it delivers a list of the detection, graph are made with any program language able to handle the data.

3.3 Two-Photon Imaging Setup

For the Two-photon imaging process we no longer have spatial information about the *signal* photon after it interacts with the mask

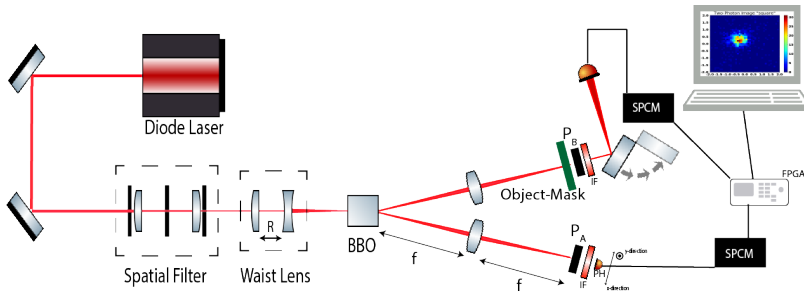


FIGURE 3.11: Experimental Setup for the Two-photon Imaging

3.3.1 Mask

This is an obstruction that is placed in the *signal* path with certain shape, it could be a mask with the shape of a letter or any other geometry. This is the object of which we want to construct an image.

3.3.2 Folding Mirror

In order to change the path followed by the *signal* photon, we use a Folding mirror, Figure 3.12. This mirror can be in the *signal* path or not.

3.3.3 Bucket Detector

This detector consists in a coupling lens that collects all the light that goes through the mask. In contrast to the other detections made in this experiment, the Bucket detector loses track of any spatial information of the *signal* photon. Another big difference is that this Bucket detector uses a multimode optic fiber to take the light to the SPCM.



FIGURE 3.12: Foldind Mirror, it is in the position for measuring the correlations

Chapter 4

Results

4.1 Achiving a Gaussian Beam

here comes de data od the new laser

4.2 Finding The Correlated Photons

SPDC nocolinear type II

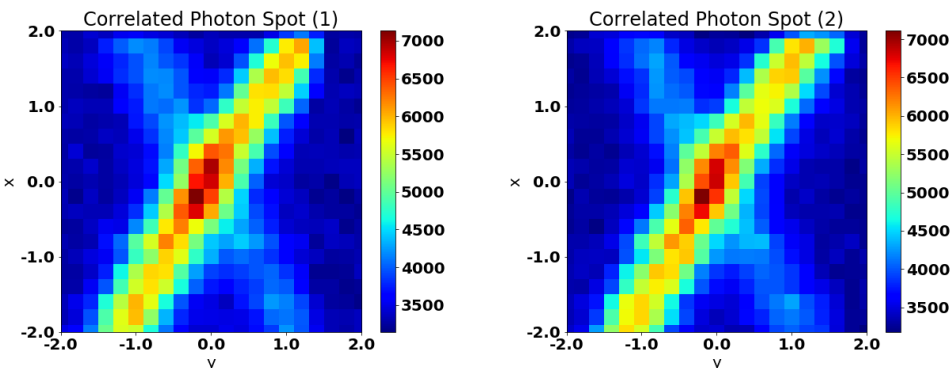


FIGURE 4.1: We are moving the translational translational stage, to locate the spot where the correlated photon are, for this try me moved the y direction

4.3 Experimental Correlations

Info taken before me

4.3.1 $w_p = ?$

4.4 Mask Alignment

We want that most of the correlated photon hits the mask
changing to the mask with an L
Long Exposure

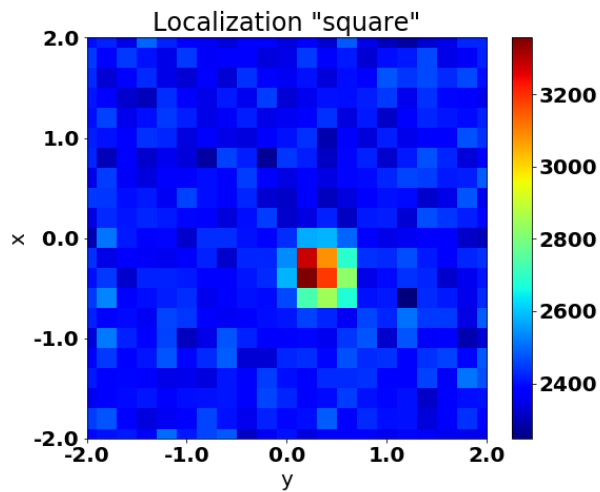


FIGURE 4.2: Localization of the mask with an square

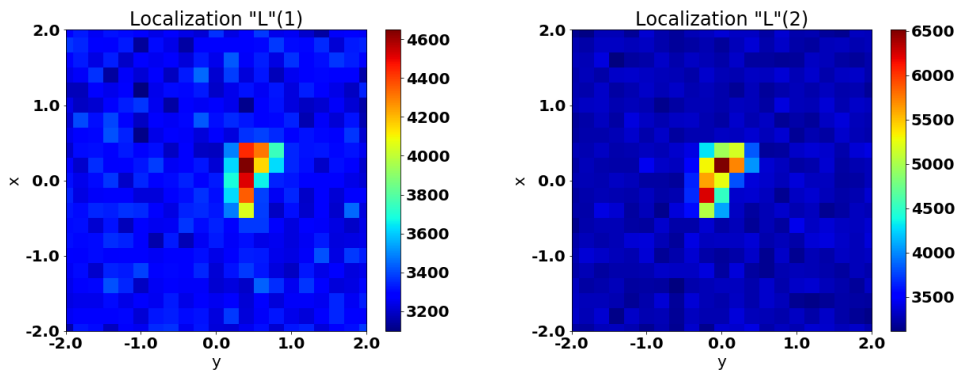


FIGURE 4.3: Moving the L Mask in order to put it in the most central spot

4.5 Two-Photon Images

4.5.1 mask1

4.5.2 mask2

4.5.3 mask3

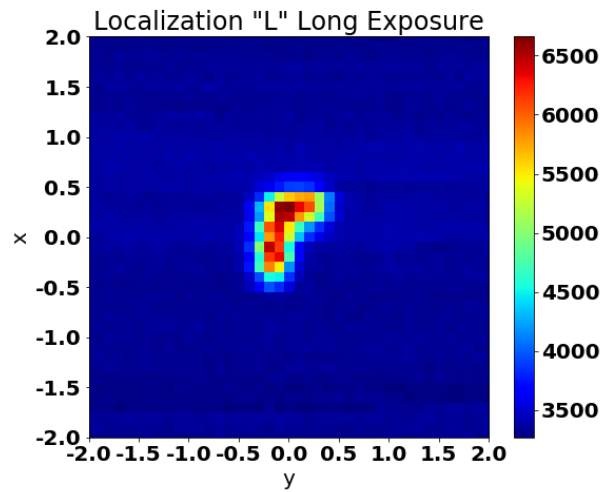


FIGURE 4.4: Long exposure of the definitive localization of the mask, in this try we leave the detector in each place for 30 seconds, we also make the steps of the detector smaller, 0.1mm

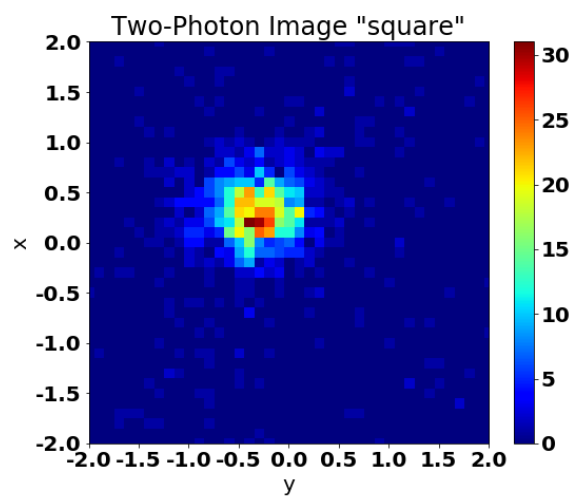


FIGURE 4.5: Localization of the mask with an square

Chapter 5

Discussions and Conclusion

Bibliography

- [1] T B. Pittman, Yanhua Shih, D V. Strekalov, and Alexander Sergienko. Optical imaging by means of two-photon quantum entanglement. *Physical review. A*, 52:R3429–R3432, 12 1995.
- [2] Crystal laser. <http://www.crystalaser.com>. Accessed: 2018-03-09.
- [3] Thorlabs, inc. <https://www.thorlabs.com/index.cfm>. Accessed: 2018-03-09.
- [4] Jeffrey H. Shapiro and Robert W. Boyd. The physics of ghost imaging. *Quantum Information Processing*, 11(4):949–993, Aug 2012.
- [5] E. Hecht. *Optics*. Pearson education. Addison-Wesley, 2016.
- [6] W. Martienssen and E. Spiller. Coherence and fluctuations in light beams. *American Journal of Physics*, 32(12):919–926, 1964.
- [7] Alejandra Valencia, Giuliano Scarcelli, Milena D’Angelo, and Yanhua Shih. Two-photon imaging with thermal light. *Phys. Rev. Lett.*, 94:063601, Feb 2005.
- [8] J.H. Shapiro. Computational ghost imaging. *Phys. Rev. A*, 78(6):061802, December 2008.
- [9] A. Einstein, B. Podolsky, and N. Rosen. Can quantum-mechanical description of physical reality be considered complete? *Phys. Rev.*, 47:777–780, May 1935.
- [10] Clara I Osorio, Alejandra Valencia, and Juan P Torres. Spatiotemporal correlations in entangled photons generated by spontaneous parametric down conversion. *New Journal of Physics*, 10(11):113012, 2008.
- [11] Jefferson Flórez, Omar Calderón, Alejandra Valencia, and Clara I. Osorio. Correlation control for pure and efficiently generated heralded single photons. *Phys. Rev. A*, 91:013819, Jan 2015.
- [12] Omar Calderón-Losada, Jefferson Flórez, Juan P. Villabona-Monsalve, and Alejandra Valencia. Measuring different types of transverse momentum correlations in the biphoton’s fourier plane. *Opt. Lett.*, 41(6):1165–1168, Mar 2016.
- [13] Y. Shih. *An Introduction to Quantum Optics: Photon and Biphoton Physics*. Series in Optics and Optoelectronics. Taylor & Francis, 2011.
- [14] Morton H. Rubin. Transverse correlation in optical spontaneous parametric down-conversion. *Phys. Rev. A*, 54:5349–5360, Dec 1996.
- [15] PerkinElmer. *Single Photon Counting Modules – SPCM*, 2010. Rev. 1.